Proceedings of the XVII ECSMGE-2019
Geotechnical Engineering foundation of the future
ISBN 978-9935-9436-1-3

doi: 10.32075/17ECSMGE-2019-0409

XVII European Conference
ECSMGE 2019
Reykjavik
on Soil Mechanics
and Geotechnical Engineering

A new approach to characterise the benefit of multi-axial geogrid on soil

Une nouvelle approche pour caractériser les avantages de la géogrille multiaxiale sur le sol

A. S. Lees
Tensar International, Nicosia, Cyprus

J. Clausen
Aalborg University, Aalborg, Denmark

ABSTRACT: The conventional approach to characterising the mechanical effect of multi-axial geogrid on soil involves testing and parameterising the mechanical properties of the soil and geogrid separately. As a result, applications of multi-axial geogrid tend to be simulated as soil plus a tensile membrane to represent the geogrid. This can lead to significant under-prediction of geogrid performance since only the reinforcement and tension membrane functions of the geogrid are taken into account. There is now a wealth of evidence to demonstrate that geogrid improves the mechanical properties of a soil by restricting the movement of its particles. This paper summarises some of the evidence and presents a new shear strength criterion derived from large triaxial compression tests performed on soil with geogrid. Implementation of this strength criterion in a finite element analysis program is used to back-analyse triaxial compression tests and a full-scale field test to demonstrate significantly improved predictions of mechanical behaviour.

RÉSUMÉ: L'approche classique pour caractériser l'effet mécanique de la géogrille multiaxiale sur le sol implique de tester et de paramétrer séparément les propriétés mécaniques du sol et de la géogrille. En conséquence, les applications de géogrille multiaxiale tendent à être simulées en tant que sol plus une membrane de traction pour représenter la géogrille. Cela peut entraîner une sous-estimation significative des performances de la géogrille puisque seules les fonctions de renforcement et de membrane de tension de la géogrille sont prises en compte. Il existe maintenant une foule de preuves pour démontrer que la géogrille améliore les propriétés mécaniques d'un sol en limitant le mouvement de ses particules. Cet article résume certaines des preuves et présente un nouveau critère de résistance au cisaillement dérivé de grands essais de compression triaxiale effectués sur un sol avec géogrille. La mise en œuvre de ce critère de résistance dans un programme d'analyse par éléments finis est utilisée pour analyser en arrière des tests de compression triaxiaux et un test de terrain à grande échelle pour démontrer les prévisions de comportement considérablement améliorées.

Keywords: Geogrid stabilisation; finite element analysis; constitutive modelling; working platforms; transportation geotechnics.

1 INTRODUCTION

Since the introduction of geogrids to the field of geotechnical engineering, for the purposes of design they have been characterised as a reinforcing tensile element with corresponding tensile stiffness *EA* and tensile strength (usually an *EA* value at a particular limiting strain value) which has been incorporated into analysis methods ranging from limit equilibrium to numerical analysis techniques such as finite element analysis (FEA). This approach was convenient because it already existed in other treatments of composite materials, e.g. reinforced concrete and reinforced earth (i.e. soil fill with steel strip reinforcement) and because the materials could be mechanically tested separately and combined in a relatively simple additive fashion in the analysis method.

However, at an early stage, it was found that such an approach often under-predicted the combined performance of soil and geogrid, which led some authors to conclude that geogrid offered negligible benefit (e.g. Gingery and Merry 2008, Araújo et al 2012) contrary to field and laboratory experience. Other authors have modified input parameters to improve the match between FEA outputs and test data. For instance, Hatami and Bathurst (2005) increased backfill stiffness in the simulation of mechanically stabilized walls and Perkins and Edens (2002) increased geogrid stiffness in the simulation of pavements.

Geogrids in unbound granular materials minimise the movement of particles when loads are applied to the surface – a function termed *stabilisation* (IGS, 2018). It is this function that was not captured by the conventional characterisation methods and which will be shown in this paper to account for the under-prediction of performance.

This paper focuses on multi-axial hexagonal (triangular aperture) geogrid because this geogrid was intended primarily to stabilise aggregate in all directions rather than attain a high tensile strength in air. Such geogrid suffers particularly from the conventional method of characterising geogrid performance (i.e. tensile strength and stiffness) even though it has been shown to outperform geogrids of superior tensile strength and stiffness in various applications at serviceable strain levels (e.g. Cook *et al*, 2015). Evidence for the fundamental action of stabilisation at particle scale will be presented initially, followed by the results of testing the stabilised soil mass, its representation in a constitutive model implemented into FEA and validation by test data.

2 STABILISATION (MICRO-SCALE)

Ingenious "SmartRock" devices comprising a 3D-printed angular shape typical of a crushed rock particle within which are housed instruments to record rotation, translation and orientation on three axes as described by Liu *et al* (2017). Their data are transmitted wirelessly to allow real-time particle movements within granular layers to be recorded. SmartRocks of about 35 and 60 mm size were placed at the bases of the sub-ballast and ballast layers respectively in a laboratory railway foundation set-up as shown in Figure 1. A vertical load on the rail was cycled at 1 Hz between 0 and 85 kN for 1,000 cycles and then for a further 1,000 cycles between 0 and 130 kN. The relatively short duration of the tests was not intended to replicate the life of a railway foundation, of course, but merely to generate particle movement of a magnitude comparable with field conditions in order to determine the influence of geogrid on this movement.

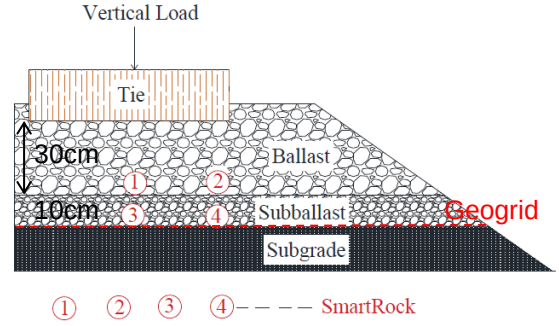

Figure 1. SmartRock test set-up

The test was performed with a stiff, polypropylene (PP), punched and drawn geogrid of a multi-axial then biaxial type installed on top of the subgrade and then repeated without any geogrid, as described by Liu *et al* (2017). As well as sleeper, or tie, settlement, movement of the SmartRocks was recorded in order to assess the effect of the geogrid on both particle movement and in terms of overall performance at reducing sleeper settlement.

The recorded accumulation of permanent sleeper settlement in the three tests are compared in Figure 2. They confirm that the installation of geogrid at the interface between the subgrade and sub-ballast significantly slowed the accumulation of sleeper settlement and that the multi-axial (TX) geogrid improved performance further, particularly at the higher load level. But how did the geogrid slow down the accumulation of permanent sleeper settlement?

The recorded angular velocity about one of the axes of the SmartRocks at Locations 1 and 3 (Figure 1) are shown in Figures 3 and 4 respectively. These results were typical of those recorded in other axes and in translation as reported by Liu *et al* (2017). At Location 3, minor rotations occurred at the lower load (85 kN) but at the higher load (130 kN) large rotations of the SmartRock in the "Control" case without geogrid were recorded while significantly reduced rotations were recorded with biaxial (BX) geogrid and further reduced with multi-axial geogrid. Location 3 was immediately adjacent to the geogrid (when present) whereas Location 1 was 10 cm above the geogrid yet a significant reduction in SmartRock rotation was still observed at both load levels.

Not only did geogrid appear to restrict the rotation of adjacent particles, but the restriction appeared to be transferred through the granular material, perhaps by inter-particle interlock, to other particles situated some distance away. Thus, a layer of aggregate with restricted particle rotation was formed by the geogrid, which appeared to be enhanced further by the use of multi-axial rather than biaxial geogrid.

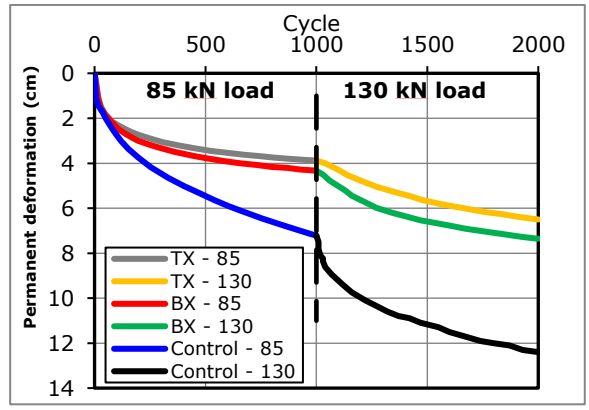

Figure 2. Measured permanent sleeper settlement in the SmartRock test set-up

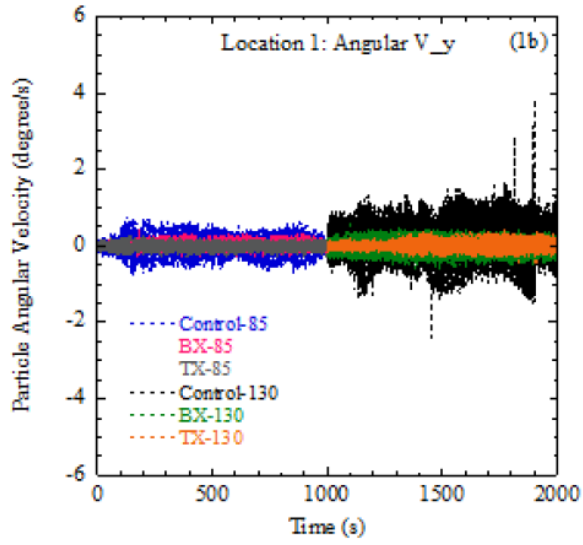

Figure 3. Recorded SmartRock angular velocity at Location 1

At a micro-scale, this is considered to be a compelling illustration of the mechanics of geogrid stabilisation. Particles interlocking with geogrid ribs were restrained against rotation and translation and the restraint was transferred some distance from the geogrid by inter-particle interlock. When particles are restrained against rotation, this increases the energy required to shear the soil. Therefore, at a macro-scale, an enhanced

shear strength of the stabilised soil mass would be expected.

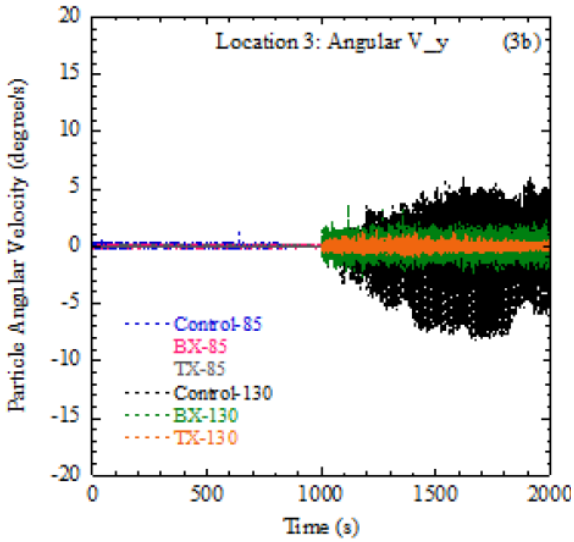

Figure 4. Recorded SmartRock angular velocity at Location 3

3 STABILISATION (MACRO-SCALE)

Very large specimen (1.0 m height x 0.5 m diameter) triaxial compression tests were undertaken on a dry, crushed diabase rock conforming to Type 1 (DoT, 2016) grading with D_{60} of 8 mm, D_{100} of 40 mm and a coefficient of uniformity C_U of 23, compacted to at least 95% maximum dry density. Tests were performed with and without a single layer of a stiff, punched and drawn multi-axial PP geogrid placed at mid-height in the specimen. Typical plots of averaged deviatoric stress q against specimen averaged axial strain ε_a at the three different vacuum-applied confining stresses shown with and without the geogrid are shown in Figure 5.

Clearly, installation of the multi-axial geogrid within the specimen resulted in a significantly increased shear strength of the combined soil and geogrid composite at all confining stress levels. Also, the enhanced strength sustained itself for significantly higher strain levels than in the non-stabilised case. Whereas post-peak shear strengths would be appropriate for many designs involving non-stabilised granular materials due to the transience of peak strengths, geogrid-stabilised peak strength could be used in many more designs due to the higher strain level to which these strength levels are sustained.

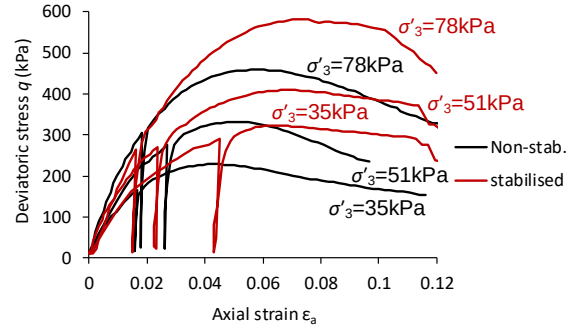

Figure 5. Large triaxial compression test data

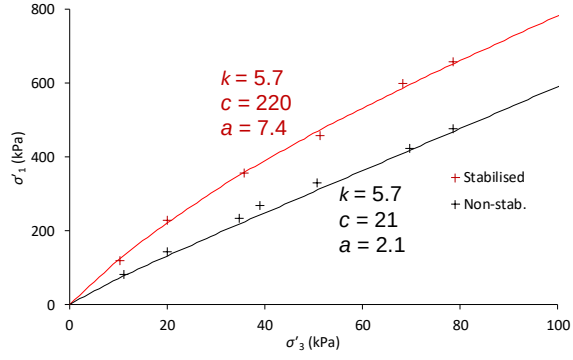

Figure 6. Peak failure stress states

Peak failure stress states on further tests on the same material at different confining stresses are plotted in terms of principle effective stresses in Figure 6. The peak strength failure envelope in the non-stabilised case is moderately curved as would be expected in a compacted, dilatant granular material. However, the stabilised failure envelope is markedly more non-linear due to the additional interlock between the aggregate particles and ribs of the geogrid. The curved envelope is a

result of the increased energy required to overcome dilation as confining stress is increased which was expected due to the restraint to the particles offered by the geogrid as shown by the SmartRock data.

4 CONSTITUTIVE MODEL

In order to characterise the constitutive behaviour of aggregates stabilised by multi-axial geogrid, three aspects of material behaviour to be included in the model were prioritised. These were as follows:

- The *effect* of geogrid on soil should be characterised by testing and modelling the stabilised soil as one composite material, so no tensile membrane elements would be used.
- A non-linear failure envelope was needed to represent shear strength accurately over a range of confining stresses.
- The strength envelope would also need to vary with distance from the geogrid plane because maximum strength occurs at the geogrid plane and it dissipates with distance until non-stabilised soil strength returns.

The failure envelope was formulated in principal stress space as defined in Equation 1 and illustrated in Figure 7. The input values to the failure envelopes fitted to the triaxial test data are also shown in Figure 6. The non-linear failure envelope is at a maximum defined by c_t and a_t at the elevation of the horizontal geogrid plane defined by the vertical axis y coordinate y_t and at a lower failure envelope defined by c_0 and a_0 beyond the zone of influence extent Δy_t of the geogrid. Both curves tend towards the same slope k which represents the inter-particle frictional component of strength. Within the influence extent, the failure envelope is interpolated between the upper and lower dependant on the perpendicular distance from y_t.

$$\sigma_1 = k\sigma_3 + c\left(1 - exp\left(-a\frac{\sigma_3}{c}\right)\right) \quad (1)$$

The prioritised aspects of behaviour were incorporated into the constitutive model as a compromise for other aspects of behaviour. Consequently, the model was formulated within a simple framework of isotropic behaviour, linear elasticity and perfect plasticity (LEPP).

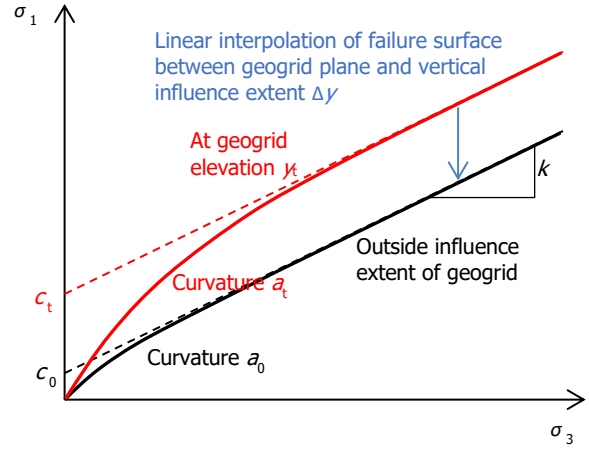

Figure 7. Non-linear failure envelopes

The constitutive model was called the Stabilised Soil (SS) model and was implemented into the Plaxis 2D 2018 geotechnical FEA software (Brinkgreve *et al*, 2018). The plastic potential was defined as shown in Equation 2 but did not vary with distance from the geogrid. m and b are generally taken as equal to k and a giving associated plasticity in non-stabilised soil but increasing non-associativity in stabilised soil.

$$\sigma_1 = m\sigma_3 + c\left(1 - exp\left(-b\frac{\sigma_3}{c}\right)\right) \quad (2)$$

Output from simulation of the same triaxial compression tests presented in Figure 5 is compared with the test data in Figures 8 and 9 for the

stabilised cases using a non-linear and linear failure envelope respectively. The non-linear failure envelope formed part of the SS model and had the input parameters shown in Table 1 while the linear Mohr-Coulomb failure envelope was used also in a LEPP model but with the non-stabilised soil parameters shown in Table 2 together with membrane elements to represent the geogrid in full frictional contact with the soil (no interface elements). A linear elastic model was used to represent the geogrid in the latter case with an isotropic axial stiffness *EA* of 360 kN/m appropriate for the strain level in the tests. The pre-failure deformation output in Figure 8 was linear due to the assumption of linear elasticity but the failure stresses were predicted well by the SS model in all cases with one set of input parameters for the failure envelope.

In contrast, the failure stresses were significantly under-predicted when using the LEPP Mohr-Coulomb model with membrane elements as shown in Figure 9. Indeed, initial failure was predicted at about the same stress as in the non-stabilised case. This was because no account was taken of the additional shear strength in the soil arising from stabilisation. When modelling the soil as a continuum, the use of a membrane elements does not impart additional shear strength into the soil. The only apparent effect of the membrane element was to cause a slow increase in deviatoric stress due to radial strains mobilising tension in the membrane elements.

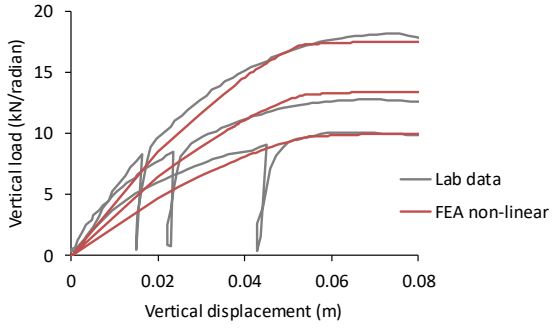

Figure 8. Triaxial test simulation output using new Stabilised Soil model with non-linear failure envelope

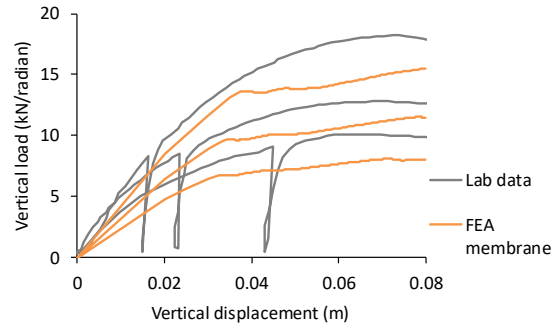

Figure 9. Triaxial test simulation output using conventional method (linear failure envelope and membrane elements for geogrid)

This simple back-analysis of the triaxial tests illustrated very well the drawback of the conventional method of testing and characterising soil and geogrid separately. The significant gain in strength of the soil stabilised by the geogrid is only taken into account by testing and characterising the materials as a single composite material.

Table 1. Input parameters to Stabilised Soil model in simulation of triaxial compression tests

Parameter	Value
k, c_0, a_0	5.7, 21kPa, 2.1
c_t, a_t, Δy_t	350kPa, 20, 0.37m
Young's modulus E	5.8, 7.8, 10MPa[†]
Poisson's ratio ν	0.1
Weight density γ	22.5kN/m^3

[†] E adjusted for confining stress.

Table 2. Input parameters to LEPP Mohr-Coulomb model in simulation of triaxial compression tests

Parameter	Value
φ', c', ψ	44.7°, 5kPa, 14.7°
Young's modulus E	5.8, 7.8, 10MPa[†]
Poisson's ratio ν	0.1
Weight density γ	22.5kN/m^3

[†] E adjusted for confining stress.

5 FULL-SCALE TEST SIMULATION

Having validated the new constitutive model by the back-analysis of triaxial tests, the performance of the new model was compared against the conventional characterisation method in the FEA-simulation of a full-scale granular platform loading test on a soft clay subgrade.

In challenging ground conditions in Port Said, Egypt comprising homogeneous deposits of alluvial clay of undrained shear strength s_u 18 kPa to at least 10 m depth, a trial working platform was constructed. The 1.1m thick platform was constructed from an uncompacted, well-graded sand and gravel of crushed rock with three layers of PP, punched and drawn multi-axial geogrid installed at 0.3, 0.7 and 1.1 m depths. The platform was loaded along a pair of 6 m by 1 m strips representing tracked plant using concrete blocks as shown in Figure 10.

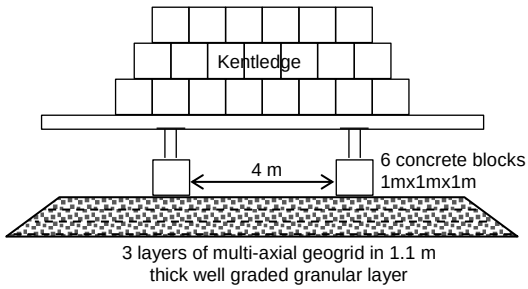

Figure 10. Full-scale stabilised platform loading test, Port Said, Egypt

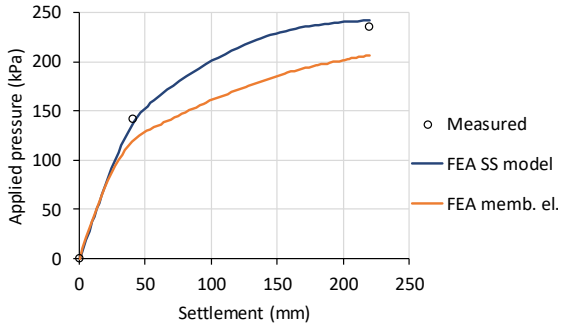

Figure 11. Full-scale stabilised platform loading test data and FEA predictions compared

The field test was simulated using Plaxis 2D FEA and a linear elastic perfectly-plastic model with Tresca yield criterion and s_u of 18 kPa and Young's modulus E of $300s_u$ to represent the natural ground. It was assumed that the geogrid placed on the ground surface contributed no additional strength to the clay which may be somewhat conservative. The working platform was modelled using both the SS model and LEPP Mohr-Coulomb model with linear elastic membrane elements to represent the geogrid. The material parameters were obtained by testing a similar granular material in the large triaxial compression apparatus described earlier in this paper.

The outputs of load and deflection from each approach are compared with the test data in Figure 11. As in the triaxial test simulation, the SS model predicts the failure load reasonably well but the LEPP Mohr-Coulomb model with membrane elements under-predicted the failure load. The geogrid benefit manifested itself only as a slow tension membrane effect as deformations continued to accumulate.

6 CONCLUSIONS

The conclusions from these studies can be summarised as follows:

- Real-time recording of particle movement during cyclic loading of granular layers showed that multi-axial geogrid is highly effective at restraining particles against translation and rotation.
- This restraint extends above and below the geogrid plane, decreasing with distance from the geogrid.
- Triaxial compression testing showed that multi-axial geogrid gave significantly higher shear strength to a granular material, which was also sustained to a higher strain level than in a non-stabilised specimen.

- A highly non-linear failure envelope is obtained for aggregates stabilised with multi-axial geogrid which has been incorporated into a new Stabilised Soil (SS) constitutive model.
- Implementation of the SS model into FEA and back-analysis of a triaxial test and full-scale working platform test showed that the new model provides much improved predictions compared with the conventional method of testing and characterising aggregate and geogrid separately.

7 ACKNOWLEDGEMENTS

The authors are grateful to Dr Mohamed El Nabarawi of AA Consultants for sharing the findings of the full-scale load test in Port Said, Egypt.

8 REFERENCES

Araújo, G.L.S., Palmeira, E.M., Macêdo, I.L. 2012. Comparisons between predicted and observed behavior of a geosynthetic reinforced abutment on soft soil, *Engineering Geology* **147-148**, 101-113.

Brinkgreve, R.B.J., Kumarswamy, S., Swolfs, W.M., Foria, F., 2018. *Plaxis 2018*. Delft.

Cook, J., Horton, M., Roe, T., Hornicek, L. 2015. Improved trackbed performance over low strength formation soils using mechanically stabilised layers, *SAICE Railway & Harbour Division Symposium*, 26-27 May, Pretoria, South Africa.

DoT. 2016. *Manual of Contract Documents for Highway Works, Volume 1 Specification for Highway Works*. Series 800. Department for Transport, UK.

Gingery, J.R., Merry, S.M. 2008. Evaluation of a geogrid-reinforced soil mat to mitigate post-liquefaction settlements – a case study. *Geotechnical Earthquake Engineering and Soil Dynamics IV* (Eds: Zeng, Manzari & Hiltunen). ASCE, Reston.

Hatami, K., Bathurst, R.J. 2005. Development and verification of a numerical model for the analysis of geosynthetic-reinforced soil segmental walls under working stress conditions, *Canadian Geotechnical Journal* **42(4)**, 1066-1085.

IGS. 2018. *Guide to the Specification of Geosynthetics*, International Geosynthetics Society, Jupiter, FL, USA.

Liu, S., Huang, H., Qiu, T. 2017. Behavior of geogrid-reinforced railroad ballast particles under different loading configurations during initial compaction phase. *Proceedings of the 2017 Joint Rail Conference*, April 4-7, Philadelphia, PA.

Perkins, S.W., Edens, M.Q. 2002. Finite element and distress models for geosynthetic-reinforced pavements, *The International Journal of Pavement Engineering* **3(4)**, 239-250.